Numerical modelling of treatment of liver metastases with irreversible electroporation

Helena Cindrič[1], Masashi Fujimori[2], Francois H. Cornelis[2, 3], Stephen B. Solomon[2, 4], Govindarajan Srimathveeravalli[2, 4], Damijan Miklavčič[1], Bor Kos[1]

[1] University of Ljubljana, Faculty of Electrical Engineering, Tržaška cesta 25, 1000 Ljubljana, Slovenia
[2] Memorial Sloan Kettering Cancer Center, Department of Radiology, 1275 York Avenue, 10065 New York, USA
[3] Sorbonne Université, ISCD, Tenon Hospital, 4 rue de la Chine, 75020 Paris, France
[4] Weill Cornell Medical College, 1300 York Avenue, 10065 New York, NY, USA
E-mail: helena.cindric@fe.uni-lj.si

Abstract. *Irreversible electroporation (IRE) has seen increasing use for ablation of deep-seated tumors, for example in the liver. A previously designed numerical framework for planning electroporation-based treatments was supplemented with computations of tissue heating and statistical probability of cell death. The frameworks' capability of predicting IRE treatment outcome was evaluated in a retrospective manner through numerical reconstruction of nine clinical cases of liver metastases treated with IRE. Patient-specific models were developed and simulations of treatments were performed. Computed results corresponded well with clinical findings predicting undertreatment in all cases where tumor recurred. Furthermore, due to a high number of delivered pulses during IRE treatment thermal damage was observed in a significant volume of modelled target tissue, indicating that current protocols used for IRE treatment may result in undesired thermal damage that may adversely affect treatment safety.*

1 Introduction

Electroporation is a phenomenon where short high voltage electric pulses are applied to biological cells (biological tissue) in order to induce structural changes in the cell membranes. Electroporation can be reversible (RE), where cells recover completely, or irreversible (IRE), where changes in the membrane result in cells' loss of functionality which can lead to apoptotic cell death [1]. Poration level mainly depends on the applied electric field strength and duration and can therefore be controlled through adjusting the applied pulse parameters – applied voltage (pulse amplitude), pulse number, duration and delivery dynamics.

RE and IRE have shown potential for use in various fields – from medicine to biotechnology and food processing [2]–[4]. In the last two decades, IRE is being evaluated for ablation of deep-seated tumors such as in liver, pancreas, prostate and kidney [5], [6]. It presents an alternative to established thermal ablation technologies due to its' predominantly non-thermal mechanism of cell kill and is currently mostly used for treating patients where the application of thermal ablation is contraindicated due to risk of thermal damage to sensitive nearby structures, or when the presence of heat sinks reduces ablation efficacy.

Since IRE is still an early technology, there is a lack of standardized treatment protocols and planning procedures for use in clinical setting. Typically a high number pulses (70-100 or even higher) is delivered per electrode pair, with an approximately 1500 V/cm voltage-to-distance ratio. The number of electrodes, electrode spacing, pulse length and delivery dynamics vary significantly between studies.

Despite IRE being considered a non-thermal technology, recent studies have shown a significant accumulation of thermal energy in the immediate vicinity of the electrodes, which if neglected in clinical setting, may affect safety of IRE treatment [7]–[9].

Numerical modelling has proven to be a fundamental tool in investigating and designing electroporation-based treatments. In light of recent studies on thermal effects of IRE, the aim of this study was to improve the existing numerical framework for planning IRE ablation of liver metastases by adding computations of temperature dissipation during treatment and statistical probability of cell kill. The improved numerical framework was validated through a retrospective analysis of nine clinical cases of liver metastases treated with IRE.

2 Materials and methods

A previously designed numerical framework for planning electroporation-based treatments [9]–[11] was supplemented with computations of tissue heating and statistical probability of cell death. The frameworks' capability of predicting IRE treatment outcome was evaluated in a retrospective manner through numerical reconstruction of nine clinical cases of liver metastases treated with IRE. The patient study was performed under a HIPPA compliant, IRB approved protocol.

2.1 Numerical framework

Current numerical models of electroporation are based on solving the stationary Laplace partial differential equation for electric potential V (Eq. 1):

$$-\nabla(\sigma \cdot \nabla \mathrm{V}) = 0 \tag{1}$$

$$\sigma \rightarrow \sigma(E) \tag{2}$$

Electroporation is implemented in the model through an electric field dependent non-linear increase in tissue electrical conductivity (Eq. 2). In short, after tissue becomes reversibly electroporated (electric field strength exceeds the threshold for RE), initial electrical conductivity of tissue increases, depending on local electric field strength *E*. The maximum conductivity value is reached if electric field strength reaches or exceeds the threshold for IRE [12]. Electric field is calculated separately for each active electrode pair, their respective contributions then combined into final electric field distribution (tissue coverage).

In IRE a large number of pulses is delivered to target tissue resulting in a significant increase in temperature (*T*). The existing stationary model of electroporation was supplemented with the Pennes bioheat transfer equation (Eq. 3) solved in time domain

$$\rho C_p \frac{\partial T}{\partial t} - \nabla(k\nabla T) = Q_{bio} + Q_h \quad (3)$$

$$Q_h = \sigma(|E|^2) \quad (4)$$

where ρ is tissue density, C_p is tissue thermal capacity and k thermal conductivity. Tissue heating from the electrodes is introduced through a Joule heating term Q_h (Eq. 4). The bioheat source term Q_{bio} (Eq. 3) represents blood perfusion and metabolic activity, however when electroporation occurs tissue perfusion decreases significantly due to vascular lock effect [13]. A rise in temperature also affects tissue electrical conductivity. Temperature dependence of electrical conductivity was modelled uniformly for all tissues with a factor of increase +1%/°C. Electrical and thermal properties of tissues were taken from the literature [9], [10], [14] and are summarized in Table 1.

Models of statistical probability of cell kill were also added to the framework to offer additional insight into treatment outcome. Probability of cell kill due to IRE was calculated with the statistical Peleg-Fermi model [15], which takes into account local electric field *E* and number of applied pulses *n*:

$$P(E,n) = 1 - \frac{1}{1 + e^{\frac{E - E_C(n)}{A_n(n)}}} \quad (5)$$

where E_c is the critical electric field causing the death of 50 % of cells, and A_n is the kinetic constant; both values were adapted from literature [8], [16]. Parameter A_n was slightly modified to better reflect the conditions in tissue.

The extent of thermal damage was determined by solving the Arrhenius kinetics equation [8]:

$$\Omega(t) = \int_{t=0}^{t=\tau} \zeta \cdot \exp\left(\frac{-A_e}{R \cdot T(t)}\right) dt \quad (6)$$

where ξ represents the frequency factor, A_e activation energy and R is the gas constant. Thermal cell kill probability was calculated with the following equation:

$$P_T = 1 - \exp(-\Omega(t)) \quad (7)$$

COMSOL Multiphysics (COMSOL Inc., Sweden) software for finite-element based analysis was used for the computations. The model set-up and computations were controlled in MATLAB (MathWorks, USA) scripting environment through LiveLink.

2.2 Reconstruction of clinical cases

The developed model was validated through a numerical reconstruction of nine clinical cases of colorectal liver metastases treated with IRE and a retrospective analysis of predicted and actual treatment outcomes.

For each patient case two sets of medical images were used for model construction – pre-interventional contrast enhanced computed tomography (CT) image, used for target tissue segmentation, and interventional CT showing electrode positions. ITK-SNAP, an open-source interactive software, was used for image registration and segmentation [17]. First both images had to be registered into a common coordinate system. The built-in function for rigid registration was used for initial registration (with mutual information as similarity criterion) and was then corrected manually to ensure the best local registration. Segmentation of target tissues – tumor volume, liver parenchyma and large adjacent blood vessels (up to 3 cm from tumor surface) – was performed manually on pre-interventional CT. Interventional CT was used to determine the points of the electrodes and their retraction trajectories (where applicable).

Segmentation masks were imported into MATLAB workspace where a patient-specific anatomically correct 3D model was built (Figure 1). Needle electrode models were added to the model geometry based on their positions determined from patient images. IRE treatment course was reconstructed using the parameters and data from NanoKnife pulse generator, namely active electrode pairs, applied pulse parameters and current/voltage measurements.

Table 1: Electrical and thermal properties of modelled biological tissues

Tissue	**Initial el. conductivity (S/m)**	**Increased el. conductivity (S/m)**	**Threshold for RE (V/cm)**	**Threshold for IRE (V/cm)**	**Tissue density (kg/m^3)**	**Heat capacity (J/kgK)**	**Thermal conductivity (W/mK)**
Tumor	0,4	1,60	400	800	1079	3540	0,52
Liver	0,091	0,45	460	700	1079	3540	0,52
Vessels	0,7	1,05	400	1100	1060	3840	/

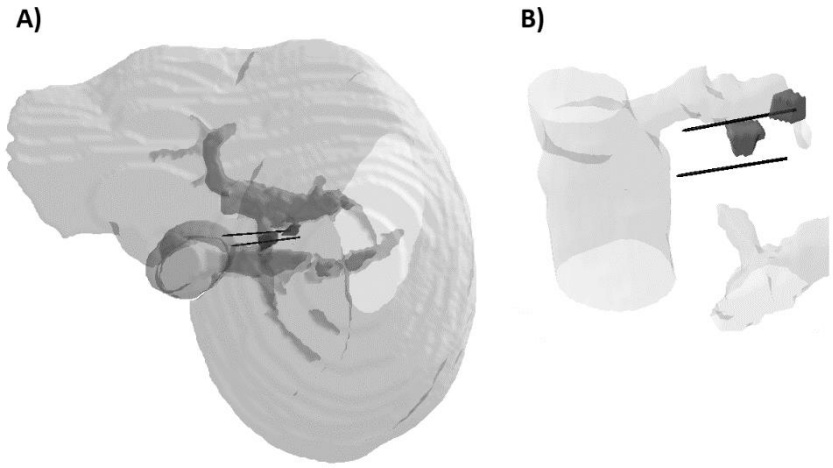

Figure 1: A) Reconstructed patient-specific numerical model showing the liver organ, major blood vessels, tumor volume and two needle electrodes. B) Close-up of the model: tumor (dark mass) is situated near a major blood vessel. IRE was performed using two needle electrodes.

Computations of electric field distribution, tissue heating and cell kill probability due to IRE and thermal damage were performed for each case. Regions of undertreatment were identified in the simulated results and then compared to clinical outcomes. The extent of possible thermal damage around the electrodes was also determined.

3 Results and discussion

The first rough estimation of the models' accuracy was performed through pair-by-pair comparison of calculated and measured electric current . This type of comparison is commonly used for verification in numerical studies [11]. The relative current error was below 30 % for most electrode pairs, with a few exceptions, presumably due to unavoidable errors in segmentations and electrode placement as well as uncertainties in electrical properties of modelled tissues.

Computed treatment outcome was evaluated based on coverage of tumor volume with sufficiently high electric field as well as cell kill probability. The exact threshold for IRE of tumor tissue has not yet been determined, however, studies report values for healthy liver tissue spanning between 500-650 V/cm for 90 (100 µs) pulses per electrode pair [9], [18]. In our computations tumor tissue ablation was considered successful if local electric field strength exceeded the assumed threshold of 500 V/cm. Furthermore, calculated probability of cell kill in ablated tissue should be at least 0.9.

Computed results for all nine reconstructed cases are presented in Table 2 along with clinical findings for each case. In eight cases out of nine tumor appeared completely ablated in follow-up images, however in four cases the tumor recurred during the two year follow-up. In one case (P4 in Table 2) undertreatment was evident already immediately after the procedure due to difficult access to the tumor site. The remaining four cases reported successful tumor ablation.

Thermal damage was observed in a significant volume of the target tissue, especially in cases where a higher number of electrodes (electrode pairs) was used for treatment. According to computations in average 30-50 % of tumor volume was thermally damaged while in two cases the extent of thermal damage reached 90 % of tumor volume. However, the volume of cell kill caused by thermal damage is always "encapsulated" within the volume of cell kill due to IRE [8], which indicates that the success of IRE treatment is not dependent on thermal damage.

Overall, computations correspond quite well with clinical findings, predicting undertreatment in areas where tumors recurred. However, computations predicted complete ablation in two of five cases in which the treatment actually failed (P1 and P3, 2. Tumor). Upon inspection of follow-up images for case P1, the site of tumor recurrence matched the area of tumor volume that was not covered in simulations (5 %). In case P3, 2. tumor, the patient had two tumors and it was unclear on follow-up images (due to local abscess) where the tumor recurred and why. In four successful cases tumor coverage varied between 80 % and 100 %, however the percentage of tumor volume in which the statistical model of IRE predicted cell death was above 95 % in all cases.

Table 2: Computation results for nine tumor cases – percentage of tumor volume covered with electric field above 500 V/cm, percentage of tumor cell kill caused by IRE and by thermal damage.

Case	Tumor coverage (%)	IRE cell kill (%)	Thermal cell kill (%)	Clinical outcome
P1	94,6	93,6	86,7	Tumor recurrence
P2	59,3	55,7	51,9	Tumor recurrence
P3, 1. tumor	71,3	79,5	59,3	Tumor recurrence
P3, 2. tumor	88,0	97,0	45,7	Tumor recurrence
P4	75,4	60,9	0,00	Confirmed undertreatment
P5	98,7	95,8	68,6	Successful ablation
P6	87,1	95,4	35,2	Successful ablation
P7, 1. tumor	81,4	95,6	29,9	Successful ablation
P7, 2. tumor	99,5	99,5	90,6	Successful ablation

Probability of cell death takes into account cumulative contributions from separate electrode pairs, resulting in higher percentage of cell kill than electric field alone.

The main limitations of this study stem from the uncertainties of electrical and thermal properties of various biological tissues especially during exposure to high electric fields. Furthermore, although numerical reconstruction of clinical cases offers further insight and analysis of various aspects of electroporation-based treatments, it is a very difficult process that is limited by the retrospective nature of available data.

4 Conclusions

Despite some limitations of our study, the presented results demonstrate the ability of our numerical framework to predict treatment outcome following IRE of liver metastases. Furthermore, we have highlighted the problem of undesired thermal effects that can occur with IRE treatment. More specifically, IRE protocols currently used in clinical setting allow for a high number of pulses to be delivered to electrode pairs, which may negatively impact treatment safety. Validated standardized protocols and treatment planning procedures for IRE are thus needed in the future.

Acknowledgements

This study was funded by the Slovenian Research Agency (P2-0249, Z3-7126) and US-Slovenian joint project (BI-US/18-19-002). The research was conducted in the scope of LEA-EBAM and MRIC UL IP-0510.

Literature

[1] T. Kotnik, P. Kramar, G. Pucihar, D. Miklavcic, and M. Tarek, "Cell membrane electroporation- Part 1: The phenomenon," *IEEE Electr. Insul. Mag.*, vol. 28, no. 5, pp. 14–23, Sep. 2012.

[2] M. L. Yarmush, A. Golberg, G. Serša, T. Kotnik, and D. Miklavčič, "Electroporation-based technologies for medicine: principles, applications, and challenges," *Annu. Rev. Biomed. Eng.*, vol. 16, pp. 295–320, Jul. 2014.

[3] T. Kotnik, W. Frey, M. Sack, S. Haberl Meglič, M. Peterka, and D. Miklavčič, "Electroporation-based applications in biotechnology," *Trends Biotechnol.*, vol. 33, no. 8, pp. 480–488, Aug. 2015.

[4] S. Mahnič-Kalamiza, E. Vorobiev, and D. Miklavčič, "Electroporation in Food Processing and Biorefinery," *J. Membr. Biol.*, vol. 247, no. 12, pp. 1279–1304, Dec. 2014.

[5] M. R. Meijerink, H. J. Scheffer, and G. Narayanan, Eds., *Irreversible Electroporation in Clinical Practice*. Springer International Publishing, 2018.

[6] H. J. Scheffer *et al.*, "Colorectal liver metastatic disease: efficacy of irreversible electroporation—a single-arm phase II clinical trial (COLDFIRE-2 trial)," *BMC Cancer*, vol. 15, Oct. 2015.

[7] E. M. Dunki-Jacobs, P. Philips, and R. C. G. Martin, "Evaluation of thermal injury to liver, pancreas and kidney during irreversible electroporation in an in vivo experimental model," *Br. J. Surg.*, vol. 101, no. 9, pp. 1113–1121, Aug. 2014.

[8] P. A. Garcia, R. V. Davalos, and D. Miklavcic, "A numerical investigation of the electric and thermal cell kill distributions in electroporation-based therapies in tissue," *PloS One*, vol. 9, no. 8, p. e103083, 2014.

[9] B. Kos, P. Voigt, D. Miklavcic, and M. Moche, "Careful treatment planning enables safe ablation of liver tumors adjacent to major blood vessels by percutaneous irreversible electroporation (IRE)," *Radiol. Oncol.*, vol. 49, no. 3, pp. 234–241, Sep. 2015.

[10] D. Šel, D. Cukjati, D. Batiuskaite, T. Slivnik, L. M. Mir, and D. Miklavčič, "Sequential finite element model of tissue electropermeabilization," *IEEE Trans. Biomed. Eng.*, vol. 52, no. 5, pp. 816–827, May 2005.

[11] D. Miklavčič *et al.*, "Towards treatment planning and treatment of deep-seated solid tumors by electrochemotherapy," *Biomed. Eng. OnLine*, vol. 9, p. 10, Feb. 2010.

[12] N. Pavšelj, Z. Bregar, D. Cukjati, D. Batiuskaite, L. M. Mir, and D. Miklavčič, "The course of tissue permeabilization studied on a mathematical model of a subcutaneous tumor in small animals," *IEEE Trans. Biomed. Eng.*, vol. 52, no. 8, pp. 1373–1381, Aug. 2005.

[13] T. Jarm, M. Cemazar, D. Miklavcic, and G. Sersa, "Antivascular effects of electrochemotherapy: implications in treatment of bleeding metastases," *Expert Rev. Anticancer Ther.*, vol. 10, no. 5, pp. 729–746, May 2010.

[14] M. Trujillo and E. Berjano, "Review of the mathematical functions used to model the temperature dependence of electrical and thermal conductivities of biological tissue in radiofrequency ablation," *Int. J. Hyperth. Off. J. Eur. Soc. Hyperthermic Oncol. North Am. Hyperth. Group*, vol. 29, no. 6, pp. 590–597, Sep. 2013.

[15] A. Golberg and B. Rubinsky, "A statistical model for multidimensional irreversible electroporation cell death in tissue," *Biomed. Eng. OnLine*, vol. 9, p. 13, Feb. 2010.

[16] J. Dermol and D. Miklavčič, "Mathematical Models Describing Chinese Hamster Ovary Cell Death Due to Electroporation In Vitro," *J. Membr. Biol.*, vol. 248, no. 5, pp. 865–881, Oct. 2015.

[17] P. A. Yushkevich *et al.*, "User-guided 3D active contour segmentation of anatomical structures: significantly improved efficiency and reliability," *NeuroImage*, vol. 31, no. 3, pp. 1116–1128, Jul. 2006.

[18] O. Gallinato, B. D. de Senneville, O. Seror, and C. Poignard, "Numerical workflow of irreversible electroporation for deep-seated tumor," *Phys. Med. Biol.*, vol. 64, no. 5, p. 055016, Mar. 2019.